Speckle Noise Reduction in Ultrasound Imaging using the Key Points in Low Degree Unbiased FIR Filters

Luis Javier Morales-Mendoza[1], René Fabián Vázquez-Bautista[1], Efrén Morales-Mendoza[1], and Yuriy Semenovich Shmaliy[2]

[1] Universidad Veracruzana, Poza Rica Ver., Mexico

[2] Universidad de Guanajuato, Salamanca Gto., Mexico

{javmorales, favazquez, efmorales}@uv.mx, shmaliy@salamanca.ugto.mx

Abstract. In this paper we present a method of reducing speckle noise in applications for ultrasound image processing using low degree unbiased FIR filters. An important feature of the p-lag gain of unbiased FIR filters is that at some cross points it converges to the reduced degree gain. The results are evaluated in terms of the signal-to-noise ratio (SNR) and the root mean square error (RMSE) metrics. We show that ultrasound image enhancing with different degree FIR filters at special lags allows getting best results depending on applications.

Keywords. FIR filters, ultrasound image, cross points.

Reducción del ruido speckle en imágenes de ultrasonido usando puntos de cruce en filtros FIR sin desplazamiento de orden bajo

Resumen. En este artículo, presentamos un método para reducir el ruido speckle en el procesamiento de imágenes de ultrasonido usando los filtros FIR sin desplazamiento de orden bajo. Una característica importante de la ganancia de los filtros FIR sin desplazamiento con paso-p es que en algunos puntos de cruce de la ganancia converge a una ganancia de grado inferior. Los resultados son evaluados en términos de las métricas de la relación señal-a-ruido (SNR) y del error cuadrático medio (RMSE). Se muestra que la imagen de ultrasonido mejorada por los filtros FIR de paso-p con diferentes grados de aproximación permite obtener mejores resultados en función de las aplicaciones.

Palabras clave. Filtros FIR, imagen de ultrasonido, puntos de cruce.

1 Introduction

The problem of saving a sharp edge with a simultaneous enhancing in images is typical for image processing. An overall panorama of nonlinear filtering following the median strategy has been given by [9] along with important modifications for a large class of nonlinear filters employing the order statistics. The algorithm issues for the filter design have been discussed in [5]. In [1], the finite impulse response (FIR) median hybrid filters (MHF) strategy has been proposed with applications to image processing. An important step ahead has been made in [4], where FIR MHF structures have been designed. In the sequel, MHF structures have been extensively investigated, developed, and used by many authors.

Basically, hybrid FIR structures can be designed using different types of estimators. Among possible solutions, polynomial estimators occupy a special place, since the polynomial models often formalize a priori knowledge about different processes well. Relevant signals are typically represented with degree polynomials to fit a variety of practical needs. Examples of applications of polynomial structures can be found in signal processing [3], timescales and clock synchronization [11], image processing [2], etc.

The polynomial estimators suitable for such structures can be obtained from the generic form of the p-step predictive unbiased FIR filter proposed by [12]. Such estimators usually

process data on finite horizons of N points which typically obtain a nice restoration.

2 Polynomial Image Model

A two-dimensional image is often represented as a $k_c \times k_r$ matrix $\mathbf{M} = \{\mu_{i,j}\}$. To provide two dimensional filtering, the matrix can be written in the form of a row-ordered vector or a column-ordered vector, respectively:

The filtering procedure is then often applied

$$\mathbf{x}_r = \left[\mu_{1,1} \cdots \mu_{1,k_r} \cdots \mu_{k_c,1} \cdots \mu_{k_c,k_r}\right]^T, \quad (1)$$

$$\mathbf{x}_c = \left[\mu_{1,1} \cdots \mu_{k_c,1} \cdots \mu_{1,k_r} \cdots \mu_{k_c,k_r}\right]^T. \quad (2)$$

twice, first to (1) and then to (2), or vice versa. To represent a two-dimensional electronic image with (1) and (2), one may also substitute each of the vectors with the discrete time-invariant deterministic signal x_{1n} which in turn can be modeled on a horizon of some N points in the state space. If x_{1n} projects ahead from $n - N + 1 - p$ to $n - p$, then the p-lag smoothing FIR filtering estimate can be provided at a current point n with a lag p, $p < 0$, as shown in Fig. 1. Referring to Fig. 1, a signal x_{1n} can further be projected on a horizon of N points, from $n - N + 1 - p$ to n, with the finite order Taylor series as follows

$$x_{1n} = \sum_{q=0}^{K-1} x_{(q+1)(n-N+1-p)} \frac{\tau^q (N-1+p)^q}{q!}, \quad (3)$$

where $x(q + 1)(n - N + 1 - p)$, $q \in [0, K - 1]$, can be called the signal $(q + 1)$-state at $n - N + 1 - p$, and the signal is thus characterized with K states, from 1 to K. Here, τ is the sampling time. In such a model, the k-state, $k \in [1, K]$, is determined by the time derivative of the $(k - 1)$-state, starting with $k = 2$. Therefore, most generally, we have

$$x_{kn} = \sum_{q=0}^{K-k} x_{(q+k)(n-N+1-p)} \frac{\tau^q (N-1+p)^q}{q!}. \quad (4)$$

3 Signal Model and Problem Formulation

An electronic image x_{1n} can be represented as a discrete time-invariant deterministic signal. Following [12], such a signal can be represented in a state space by the state and observation equations as follows, respectively:

$$\mathbf{x}_n = \mathbf{A}^{N-1+p} \mathbf{x}_{n-N+1-p} \quad (5)$$

$$y_n = \mathbf{C}\mathbf{x}_n + v_n, \quad (6)$$

where $\mathbf{x}_n = [x_{1n}\ x_{2n}\ \ldots\ x_{Kn}]$ is the $K \times 1$ vector of the states, y_n is the measurement representing the electronic image, v_n is the measurement noise, the $1 \times K$ measurement matrix is $\mathbf{C} = [1\ 0\ \ldots\ 0]$, and the $K \times K$ triangular matrix $\mathbf{A}^i$ is specified by

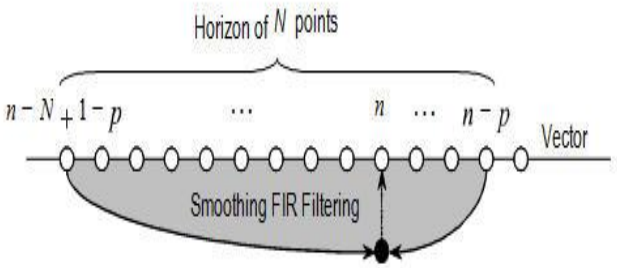

Fig. 1. Smoothing FIR filtering on a horizon of N points with a lag p, $p < 0$

$$\mathbf{A}^i = \begin{bmatrix} 1 & \tau i & \frac{1}{2}(\tau i)^2 & \ldots & \frac{1}{(K-1)!}(\tau i)^{K-1} \\ 0 & 1 & \tau i & \ldots & \frac{1}{(K-2)!}(\tau i)^{K-2} \\ 0 & 0 & 1 & \ldots & \frac{1}{(K-3)!}(\tau i)^{K-3} \\ \ldots & \ldots & \ldots & \ldots & \ldots \\ 0 & 0 & 0 & \ldots & 1 \end{bmatrix}. \quad (7)$$

Now, the noiseless model (5) projects ahead from $n - N + 1 - p$ to n with the exponential Taylor polynomial represented as

$$x_n = \sum_{q=0}^{K-1} x_{l+q} \frac{\tau^q (N-1+p)^q}{q!}. \quad (8)$$

If we introduce $h_{li}(N, p)$ as the gain of the l-degree polynomial p-step dependent filter, then the estimate of the electronic image x_{1n} can be obtained based on the averaging concept by convolution on the horizon of N points

$$\hat{x}_n = \sum_{i=p}^{N-1+p} h_{li}(N, p) y_{n-i} \ , \tag{9}$$

where the positive step, $p > 0$, is supposed for predictive FIR filtering, $p = 0$ for FIR filtering, and $p < 0$ for smoothing FIR filtering. It has been shown in [12] that for the unbiased estimate the gain $h_{li}(N, p)$ must satisfy the following conditions:

$$\sum_{i=p}^{N-1+p} h_{li}(N, p) = 1, \tag{10}$$

$$\sum_{i=p}^{N-1+p} h_{li}(N, p) i^u = 0 \quad u \in [1, \ l]. \tag{11}$$

It is known from the optimal filtering theory that the order of the optimal (and so unbiased) filter is the same as that of the system. It means that, for the K state model, the gain can be represented with the l-degree polynomial such that

$$h_{li}(N, p) = \sum_{j=0}^{l} a_{jl}(N, p) i^j \ , \tag{12}$$

where $a_{jl}(N, p)$ are the polynomial coefficients and the degree l must be chosen such that $l = K - 1$. The coefficients for the polynomial (12) have been found in [12] in the form of

$$a_{jl}(N, p) = (-1)^j \frac{M_{(j+1)1}(N, p)}{|\mathbf{D}(N, p)|} \ , \tag{13}$$

where a short $(l + 1)\times(l + 1)$ symmetric matrix $\mathbf{D}(N, p)$ is given by

$$\mathbf{D} = \begin{bmatrix} d_0 & d_1 & \cdots & d_l \\ d_1 & d_2 & \cdots & d_{l+1} \\ \vdots & \vdots & \ddots & \vdots \\ d_l & d_{l+1} & \cdots & d_{2l} \end{bmatrix}, \tag{14}$$

where $|\mathbf{D}|$ is the determinant of (14) and $M_{(j+1)1}$ is the minor of (14). In accordance with [12], the component of (14) can be determined using the Bernoulli polynomials $B_n(x)$ as follows:

$$d_r(N, p) = \frac{1}{r+1}\left[B_{r+1}(N + p) - B_{r+1}(p)\right]. \tag{15}$$

4 Noise Power Gains (NPG) of the Low Degree Polynomials

In FIR filtering, an estimate is obtained via the discrete convolution applied to measurement. That can be done if we represent the state space model on an averaging interval of some N points. Referring to (12), the low-degree polynomial gains can thus be defined by

$$h_{1i}(p) = \sum_{j=0}^{3} a_{ji}(p) i^j \ . \tag{16}$$

A model that is uniform over an averaging horizon of N points is the simplest one. The relevant signal is characterized with one state and the filter gain is represented by (9), with the 0-degree polynomial as

$$h_{0i}(p) = \begin{cases} \frac{1}{N} & p \le N - 1 + p \\ 0 & \text{otherwise} \end{cases} . \tag{17}$$

For linear models, the p-lag gain, existing from p to $N - 1 + p$, becomes ramp

$$h_{1i}(p) = a_{01}(p) + a_{11}(p) i \tag{18}$$

having the coefficients (see Appendix A, for details)

$$a_{01}(p) = \frac{2(2N - 1)(N - 1) + 12p(N - 1 + p)}{N(N^2 - 1)}, \tag{19}$$

$$a_{11}(p) = -\frac{6(N - 1 + 2p)}{N(N^2 - 1)}. \tag{20}$$

For the quadratic and cubic models, the gain of the unbiased smoothing FIR filter becomes

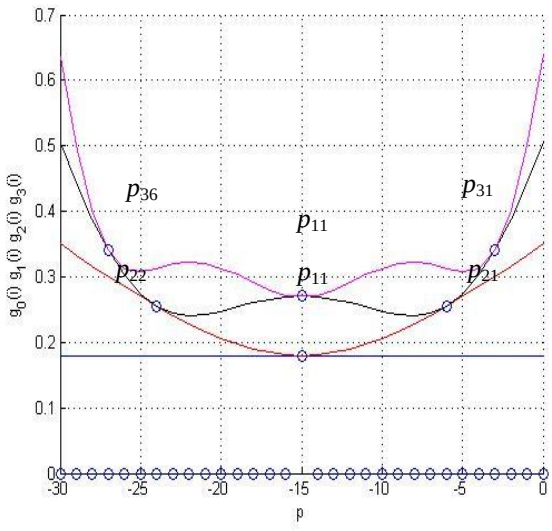

Fig. 2. Cross point between the low-degree polynomial gains for $N = 31$

$$h_{2i}(p) = a_{02}(p) + a_{12}(p)i + a_{22}(p)i^2 \qquad (21)$$

and

$$h_{3i}(p) = a_{03}(p) + a_{13}(p)i + a_{23}(p)i^2 + a_{33}(p)i^3, \qquad (22)$$

respectively, where the coefficients $a_{02}(p)$, $a_{12}(p)$, and $a_{22}(p)$ are defined in [12]; on the other hand, $a_{03}(p)$, $a_{13}(p)$, $a_{23}(p)$, and $a_{33}(p)$ are defined in [10], respectively.

5 The Cross Points of the NPG

Noise in FIR estimates is often evaluated in terms of the noise power gain (NPG) defined as follows:

$$g_l = \sum_{i=p}^{N-1+p} h_{li}^2(N, p). \qquad (23)$$

Referring to equations (17), (18), (21), and (22), see [6]. To find the cross point between the uniform gain (17) and the ramp gain (18), we solve $g_0 = g_1$ such as defined in [6, 8,10]:

$$p_{11} = -\frac{N-1}{2}. \qquad (24)$$

Similarly, the cross points of the ramp gain (18) and the quadratic gain (21) can be found. Namely, by the lags

$$p_{21} = -\frac{N-1}{2} + \sqrt{\frac{N^2-1}{12}}, \qquad (25)$$

$$p_{22} = -\frac{N-1}{2} - \sqrt{\frac{N^2-1}{12}}. \qquad (26)$$

Finally, the cross points of the gain (21) and the cubic gain (22) can be found as follows:

$$p_{31} = -\frac{N-1}{2} + \frac{1}{10}\sqrt{5\left(3N^2-7\right)}, \qquad (27)$$

$$p_{36} = -\frac{N-1}{2} - \frac{1}{10}\sqrt{5\left(3N^2-7\right)} \qquad (28)$$

6 Design and Application of the Unbiased FIR Median Hybrid (FMH) Structure

In this section, we employ the above derived p-dependent gains in order to design efficient hybrid structures suitable for nonlinear image processing. Every image is considered as an array of two signals, $\mathbf{x}_r$ and $\mathbf{x}_c$ as showed in (1) and (2), respectively, and processed as follows. First, we filter out noise in the row vector and then reconstruct the image. Next, the partly enhanced image is decomposed into the column vector, the filtering procedure is applied once again, and the fully enhanced image is reconstructed. For the sake of minimizing errors in the enhanced image,

all of the above designed low-degree polynomial gains have been examined in the FMH structure. Namely, we employ all *p*-dependent gains and the ramp gain (18)-(20). It is known that FMH structures can be designed to have *k* substructures and that a number of such substructures need to be optimized, which is a special topic. Leaving the optimization problem for further investigation, in this paper we mostly examine the basic FMH structure and demonstrate the effect of a number of sub-blocks.

The block diagram of the basic FIR median hybrid (FMH) structure was developed in [4] to maximize the SNR in the row and column vectors. Here, the input signal y_n is filtered with two FIR filters. The forward FIR filter (FIRFW) computes the points on the horizon to the left from the point n. In turn, the backward FIR filter (FIRBW) processes data on the same length horizon lying to the right from *n*. The estimates are hence formed as respectively.

$$\hat{x}_n^{FW}(p) = \sum_{i=p}^{N-1+p} h_{li}(p) y_{n-i} , \tag{29}$$

$$\hat{x}_n^{BW}(p) = \sum_{i=p}^{N-1+p} h_{li}(p) y_{n+i} , \tag{30}$$

The output signal $\hat{x}_n(p)$ is obtained using the nonlinear operator called the "median". In the median structure, the input y_n and the outputs of the FIR filters, $\hat{x}_n^{BW}(p)$ and $\hat{x}_n^{FW}(p)$, play the role of entries. Following the median filter strategy, the output $\hat{x}_n(p)$ becomes equal to the intermediate value stated by the operator

$$\hat{x}_n(p) = \mathrm{MED}\left[\hat{x}_n^{BW}(p), y_n, \hat{x}_n^{FW}(p)\right] . \tag{31}$$

Note that the best filtering result can be obtained if one sets properly the smoother lag *p* or the prediction step *p* in the FIR filters. Since the basic structure shown in [4] is commonly unable to obtain nice image enhancing owing to the small number of entries, a more sophisticated FMH structure exploiting a different *p* would provide better performance.

7 Simulations

For further investigation, we chose a renal ultrasound image of 250 × 320 pixels showed in Fig. 3. The image was contaminated with both additive white Gaussian and speckle noise components as shown in Fig. 4 [6]. The simulation conditions were taken as follows: the horizon is *N* = 31, the *p*-lag was allowed to be at the cross points of p_{11} = –15, p_{21} = –24, p_{22} = –6, p_{36} = –27, and p_{31} = –3 (see Fig. 1), and the noise variance was set as σ^2 = 0.2. To provide image enhancing, we employed median structures fitting. As it can be seen, provided *N* = 31, the best enhancing is achieved with the quadratic gain of degree *l* = 2 which is the reduced order cubic gain, *l* = 3, at the aforementioned cross points. For numerical evaluation, we apply two classical quantitative metrics: the Signal-to-Noise Ratio (SNR) and the Root-Mean-Square-Error (RMSE) metrics. The first and second metric are defined respectively as

$$SNR_{dB} = 10\log_{10}\left(\frac{\sum_{i=1}^{P}\sum_{j=1}^{Q}[x(i,j)]^2}{\sum_{i=1}^{P}\sum_{j=1}^{Q}[\hat{x}(i,j)-x(i,j)]^2}\right), \tag{32}$$

$$RMSE = \sqrt{\frac{1}{PQ}\sum_{i=1}^{P}\sum_{j=1}^{Q}[x(i,j)-\hat{x}(i,j)]^2} . \tag{33}$$

The results are sketched in Figures 5-7; we evaluate the enhancements in terms of SNR and RMSE, as shown in Table 1, at each of the cross points (Fig. 1). On the other hand, in Figures 8 and 9 we showed the enhancement of the ultrasound image for the predictive case (*p* = 1) and the filtering case (*p* = 0), respectively. In Tables 2 and 3, we present the numerical evaluation in both cases.

Table 1. Quantitative evaluation

Degree	*p*-lag	SNR (dB)	RMSE
$l = 1$	$P_{11} = -15$	**5.1189**	**8.8575**
$l = 2$	$p_{21} = -6$	**5.8962**	**8.0993**
	$p_{22} = -24$	4.3822	9.6915
$l = 3$	$p_{31} = -3$	**6.1162**	**7.8967**
	$p_{36} = -27$	4.0775	9.9857

Table 2. Quantitative evaluation with $p = 1$ [4]

Degree	SNR (dB)	RMSE
$l = 1$	**5.6656**	**8.3171**
$l = 2$	4.8519	9.1340
$l = 3$	4.1401	9.9140

Table 3 Quantitative evaluation with $p = 0$

Degree	SNR (dB)	RMSE
$l = 1$	5.8408	8.1511
$l = 2$	5.5761	8.4033
$l = 3$	**6.1162**	**7.8967**

Fig. 3. Original ultrasound image

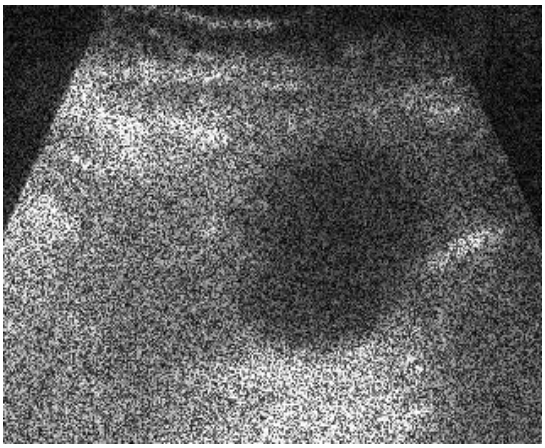

Fig. 4. Noisy Ultrasound Image with $\sigma^2 = 0.2$

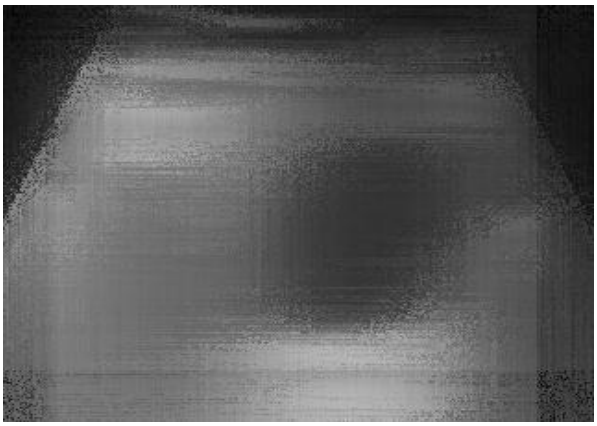

Fig. 5. Enhancing Ultrasound Image with $l = 1$ and p_{11}

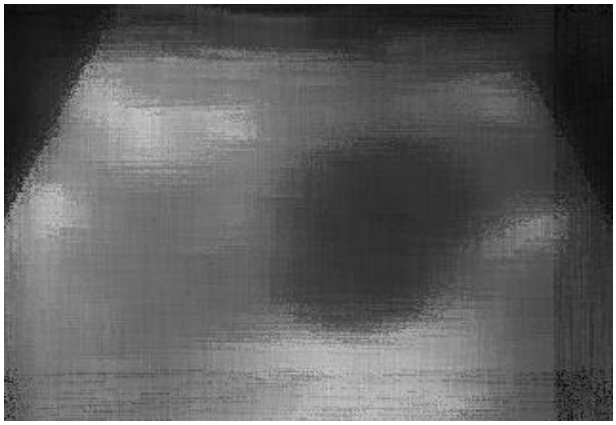

Fig. 6. Enhancing Ultrasound Image with $l = 2$ and p_{21}

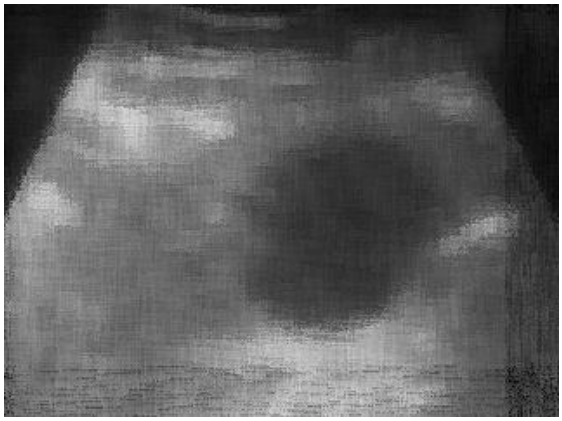

Fig. 7. Enhancing Ultrasound Image with *l* = 3, and p_{31}

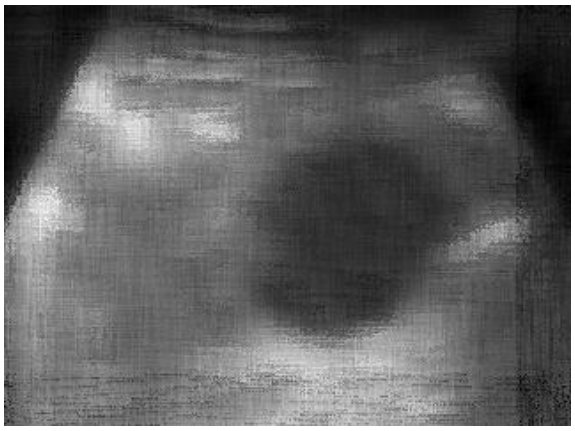

Fig. 8. Enhancing Ultrasound Image with l = 1 and p = 1

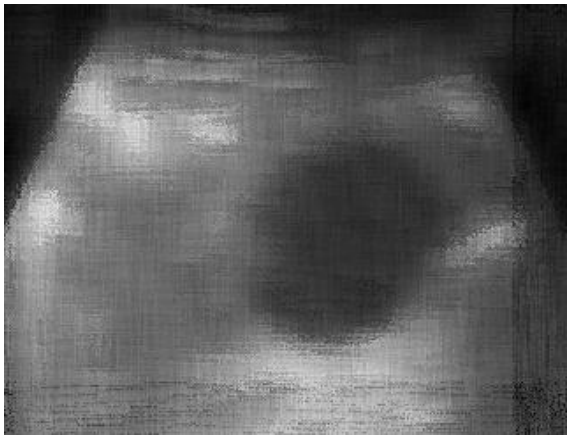

Fig. 9. Enhancing Ultrasound Image with *l* = 1 and *p* = 0

8 Conclusions

In this paper, we investigated the performance of the *p*-step unbiased smoothing FIR filter with low-degree polynomials gains at the cross points. The results are illustrated in Figures 5-7 for smoothers having different degrees and lags. Figures 8 and 9 show two particular cases of smoother with *p*=1 and *p*=0, respectively. To compare errors, Tables 1, 2 and 3 give the estimated values of the SNRs and RMSEs. The analysis shows that an increase in the smoother degree does not lead to better denoising and error reduction. On the other hand, better enhancing is achieved with the lags, allowing for reducing the smoother degree. That opens new horizons for optimization of hybrid FIR structures, which is currently under investigation.

Appendix A

To determine the response function of the ramp gain (*l* = 1), the matrix **D** coefficients are derived using (14), as follows:

$$\cdot\ \mathbf{D} = \begin{pmatrix} d_0 & d_1 \\ d_1 & d_2 \end{pmatrix} \tag{A1}$$

Here the coefficients are calculated with equation (15) based on the recurrent relation of the Bernoulli polynomial introduced by Y. S. Shmaliy [11] as follows:

$$d_0 = N \tag{A2}$$

$$d_1 = \frac{1}{2} N(N-1) + Np \tag{A3}$$

$$d_2 = \frac{1}{6} N(2N-1)(N-1) + N(N-1)p + Np^2 \tag{A4}$$

Then the determinant of matrix **D** was found by substituting (A2)-(A4) in (A1) respectively:

$$\det(\mathbf{D}) = \frac{1}{12} N^2 \left(N^2 - 1\right) \tag{A5}$$

Moreover, the minor matrices are defined as follows:

$$M_{11}(N,p)=d_2 \quad \text{(A6)}$$

$$M_{21}(N,p)=-d_1 \quad \text{(A7)}$$

Finally, the 1-degree polynomial gain can be deduced by (12) as follows:

$$h_{1i}(N,p)=a_{01}(N,p)+ia_{11}(N,p) \quad \text{(A8)}$$

where the coefficients are derived by inserting (A5)-(A7) into (13).

Acknowledgements

The first author thanks PROMEP and the FIEC – Veracruz University for the whole research support.

References

1. **Astola, J. & Kuosmanen, P. (1997).** *Fundamentals of Nonlinear Digital Filtering*. Boca Raton, Fla.: CRC Press.
2. **Bose, T. (2004).** *Digital Signal and Image Processing*. Hoboken, NJ.: J. Wiley.
3. **Dumitrescu, B. (2007).** *Positive Trigonometric Polynomials and Signal Processing Applications.*Dordrecht: Springer.
4. **Heinonen, P. & Neuvo, Y. (1988).** FIR-median hybrid filter with predictive FIR substructures. *IEEE Transactions on Acoustics, Speech, and Signal Processing*, 36(6), 892-899.
5. **Kalouptsidis, N. & Theodoridis, S. (1993).** *Adaptive system Identification and signal processing Algorithms*. New York: Prentice Hall.
6. **Morales-Mendoza, L.J, Shmaliy, Y.S., & Ibarra-Manzano, O.G. (2009).** Enhancing Ultrasound Images using Hybrid FIR Structures. *Image Processing,* 287-310, Vukovar, Croatia: InTech
7. **Morales-Mendoza, L.J. & Shmaliy, Y. (2010).** Moving Average Hybrid Filter to the Enhancing Ultrasound Image Processing. *IEEE Latin America Transactions*, 8(1), 9-16.
8. **Morales-Mendoza, L.J., Shmaliy, Y.S., & Pérez-Cáceres, S. (2010).** An analysis of cross points in the low-degree polynomial gains of p-lag unbiased smoothing FIR filters. *15th IEEE Mediterranean Electrotechnical Conference* (MELECON 2010), Valletta, Malta, 878-883.
9. **Pitas, I. & Venetsanopoulos, A.N. (1990).** *Nonlinear Digital Filters: Principles and Applications*. Boston: Kluwer Academic Publishers.
10. **Shmaliy, Y.S. & Morales-Mendoza, L.J. (2010).** FIR smoothing of discrete-time polynomial signals in state space. *IEEE Transactions on Signal Processing*, 58(5), 2544-2555.
11. **Shmaliy, Y.S. (2006).** An unbiased FIR filter for TIE model of a local clock in applications to GPS-based timekeeping. *IEEE Transactions on Ultrasonic, Ferroelectrics and Frequency Control*, 53(5), 862-870.
12. **Shmaliy, Y.S. (2009).** An unbiased *p*-step predictive FIR filter for a class of noise-free discrete time models with independently observed states. *Signal, Image & Video Processing*, 3(2), 127-135.

Luis Javier Morales-Mendoza received the B.Sc. degree in Electronics and Communications Engineering from Veracruz University in 2001, M.Sc. in Electrical Engineering from Guanajuato University, Mexico, 2002, and the Ph.D. degree in Electrical Engineering from CINVESTAV, Guadalajara, in 2006. From 2006 to 2009, he had been with the Electronics Department of Guanajuato University of Mexico as an Assistant Professor. He is currently a Professor of the FIEC of Veracruz University of Mexico. His scientific interests are in the Artificial Neural Networks applied to Optimization Problems, Image Restoration and Enhancing, and Ultrasound Image Processing. He has authored and co-authored more than 45 journal and conference papers.

René Fabian Vazquez-Bautista received the B.Sc. degree in Electronics and Communications Engineering from Veracruz University; the M. Eng. in Electrical Engineering from Guanajuato University; and the Ph.D. degree by CINVESTAV,

Guadalajara, in 2000, 2002 and 2006, respectively. From 2007 to 2009, he had been with the ITESM, Campus Guadalajara as an Assistant Professor. Nowadays, he is a full-time Professor with Veracruz University in FIEC, Campus Poza Rica. His scientific interests are Digital Signal and Image Processing, Data and Sensor Fusion, Biomedical Applications and Embedded Systems.

Efrén Morales-Mendoza received the B. Sc. degree in Electronics and Communications Engineering from Veracruz University in 1993, M. Sc. in Computer Science from the Engineering Institute of Veracruz University in 2005. Currently he holds a PhD. He studied Education at Veracruz Institute of Higher Education. Since 1995 he has been a Professor of the FIEC of Veracruz University of Mexico. His research interests are Educational Applications in Engineering, Numerical Methods for Applications in Education.

Yuriy Semenovich Shmaliy received the B.Sc., M.Sc., and Ph.D. degrees, all in Electrical Engineering, from Kharkiv Aviation Institute, Ukraine, in 1974, 1976, and 1982, respectively, and the Doctor of Technical Sc. degree from Kharkiv Railroad Institute in 1992. In March 1985, he joined Kharkiv Military University, where he had served as a full-time Professor since 1986. From 1999 to 2009, he had been with Kharkiv National University of Radio Electronics, and since November 1999 he has been a full-time Professor at Guanajuato University of Mexico. He has published 249 journal and conference papers and holds 80 patents. He also published three books: Continuous-Time Signals (Springer, 2006), Continuous-Time Systems (Springer 2007), and GPS-Based Optimal FIR Filtering of Clock Models (Nova Science Publ., 2009).

Article received on 16/11/2010; accepted on 08/02/2012.